

RESEARCH ARTICLE

TUFT1, a novel candidate gene for metatarsophalangeal osteoarthritis, plays a role in chondrogenesis on a calcium-related pathway

Eeva Sliz^{1,2,3}✉, Mari Taipale^{1,2,3}✉, Maiju Welling^{1,2,4}, Sini Skarp^{1,2,3}, Viivi Alaraudanjoki⁵, Jaakko Ignatius⁶, Lloyd Ruddock^{2,3}, Ritva Nissi⁷, Minna Männikkö^{1,2*}

1 Center for Life Course Health Research, Faculty of Medicine, University of Oulu, Oulu, Finland, **2** Faculty of Biochemistry and Molecular Medicine, University of Oulu, Oulu, Finland, **3** Biocenter Oulu, University of Oulu, Oulu, Finland, **4** Medical Research Center Oulu, Oulu University Hospital and University of Oulu, Oulu, Finland, **5** Research Unit of Oral Health Sciences, University of Oulu, University of Oulu, Oulu, Finland, **6** Department of Clinical Genetics, Turku University Hospital, Turku, Finland, **7** Department of Obstetrics and Gynecology, Oulu University Hospital, Oulu, Finland

✉ These authors contributed equally to this work.

* minna.mannikko@oulu.fi



OPEN ACCESS

Citation: Sliz E, Taipale M, Welling M, Skarp S, Alaraudanjoki V, Ignatius J, et al. (2017) *TUFT1*, a novel candidate gene for metatarsophalangeal osteoarthritis, plays a role in chondrogenesis on a calcium-related pathway. PLoS ONE 12(4): e0175474. <https://doi.org/10.1371/journal.pone.0175474>

Editor: Irina Kerkis, Instituto Butantan, BRAZIL

Received: November 23, 2016

Accepted: March 27, 2017

Published: April 14, 2017

Copyright: © 2017 Sliz et al. This is an open access article distributed under the terms of the [Creative Commons Attribution License](https://creativecommons.org/licenses/by/4.0/), which permits unrestricted use, distribution, and reproduction in any medium, provided the original author and source are credited.

Data Availability Statement: The exome data were deposited to NIH SRA with submission ID PRJNA373947, and are available from <https://trace.ncbi.nlm.nih.gov/Traces/study/?acc=SRP099181&go=go>.

Funding: This study was funded by the University of Oulu (university researcher recruitment funding, MM).

Competing interests: The authors have declared that no competing interests exist.

Abstract

Osteoarthritis (OA) is the most common degenerative joint disorder and genetic factors have been shown to have a significant role in its etiology. The first metatarsophalangeal joint (MTP I) is highly susceptible to development of OA due to repetitive mechanical stress during walking. We used whole exome sequencing to study genetic defect(s) predisposing to familial early-onset bilateral MTP I OA inherited in an autosomal dominant manner. A non-synonymous single nucleotide variant rs41310883 (c.524C>T, p.Thr175Met) in *TUFT1* gene was found to co-segregate perfectly with MTP I OA. The role of *TUFT1* and the relevance of the identified variant in pathogenesis of MTP I OA were further assessed using functional *in vitro* analyses. The variant reduced *TUFT1* mRNA and tuftelin protein expression in HEK293 cells. ATDC5 cells overexpressing wild type (wt) or mutant *TUFT1* were cultured in calcifying conditions and chondrogenic differentiation was found to be inhibited in both cell populations, as indicated by decreased marker gene expression when compared with the empty vector control cells. Also, the formation of cartilage nodules was diminished in both *TUFT1* overexpressing ATDC5 cell populations. At the end of the culturing period the calcium content of the extracellular matrix was significantly increased in cells overexpressing mutant *TUFT1* compared to cells overexpressing wt *TUFT1* and control cells, while the proteoglycan content was reduced. These data imply that overexpression of *TUFT1* in ATDC5 inhibits chondrogenic differentiation, and the identified variant may contribute to the pathogenesis of OA by increasing calcification and reducing amount of proteoglycans in the articular cartilage extracellular matrix thus making cartilage susceptible for degeneration and osteophyte formation.

Introduction

Osteoarthritis (OA) is one of the most common musculoskeletal disorders worldwide and its prevalence is predicted to increase in the future [1]. OA is a disease of the whole joint [2] and the main pathologic changes are progressive loss of articular cartilage, joint space narrowing, osteophyte formation, subchondral bone sclerosis, and cyst formation [3]. These lead to pain and loss of joint function in OA patients [4]. During the development of OA chondrocytes start to proliferate and express matrix-degrading enzymes leading to matrix remodeling involving hypertrophic maturation of chondrocytes and calcification of cartilage [5]. In general, OA is considered as a complex trait caused by interplay between genetic and environmental factors [6]. In twin studies the influence of genetic components has been predicted to be as high as 39–65% depending on joint site [7]. Although OA generally lacks a clear Mendelian pattern of inheritance, rare familial early-onset forms with autosomal dominant inheritance have been described [8–11].

Foot OA is poorly studied in comparison to hip or knee OA, although the first metatarsophalangeal (MTP I) joint is often affected by OA [12]. The prevalence of radiographic MTP I OA has been estimated to be from 6.3% to 39% in middle-aged and older adults [13]. Foot OA shares many risk factors with other forms of OA, like age and obesity. Also, mechanical stress, trauma and inflammation are often associated with foot OA [12]. Individuals with symptomatic MTP I OA experience localized pain and stiffness during movement and therefore have difficulties in various physical tasks such as walking [14].

Nissi *et al.* (2011) reported a family with early-onset bilateral foot arthritis limited to the MTP I joint [15]. The family history strongly suggests an autosomal dominant inheritance. In order to identify the genetic defect(s) predisposing to this disorder, we performed whole exome sequencing on the aforementioned family and identified a variant in *TUFT1* co-segregating with the disease. *TUFT1*, encoding tuftelin protein, is previously known to be involved in enamel mineralization [16] and is recognized as a candidate gene for dental caries [17], but is suggested to have a universal or multifunctional role due to its expression in multiple cell and tissue types [18–20]. In cartilage, *TUFT1* expression is strongest in the deeper, mineralizing zones [21]. Interestingly, *TUFT1* expression has been shown to be regulated *in vitro* by hypoxia-inducible factor 1- α and hedgehog pathways, both essential for cartilage and bone formation [22,23]. However, the precise function of tuftelin is not fully known. We show that *TUFT1* participates in regulation of chondrocyte differentiation and that the identified variant gives rise to extracellular matrix (ECM) modifications observed in association with OA. We propose that *TUFT1* is a novel candidate gene for foot OA and that the identified variant is likely to be involved in the pathogenesis of foot OA in the studied family.

Results

Whole exome sequencing

Three affected individuals from a Finnish family with MTP I OA (Fig 1) and two unrelated individuals (controls) were analyzed using whole exome sequencing. Summary of the exome sequencing and variant annotation is shown in Table 1. The three patients shared in total 48 860 single nucleotide variants (SNVs) and 4 670 insertions and deletions (indels). Following the variant filtering steps, altogether 33 SNVs and five indels (S1 Table) were selected for validation by Sanger sequencing in all nine family members whose DNA was available for the study (four affected, five unaffected, Fig 1). The variant rs41310883 (c.524C>T) in *TUFT1* was found heterozygous in all four patients, but was not detected in healthy family members, being

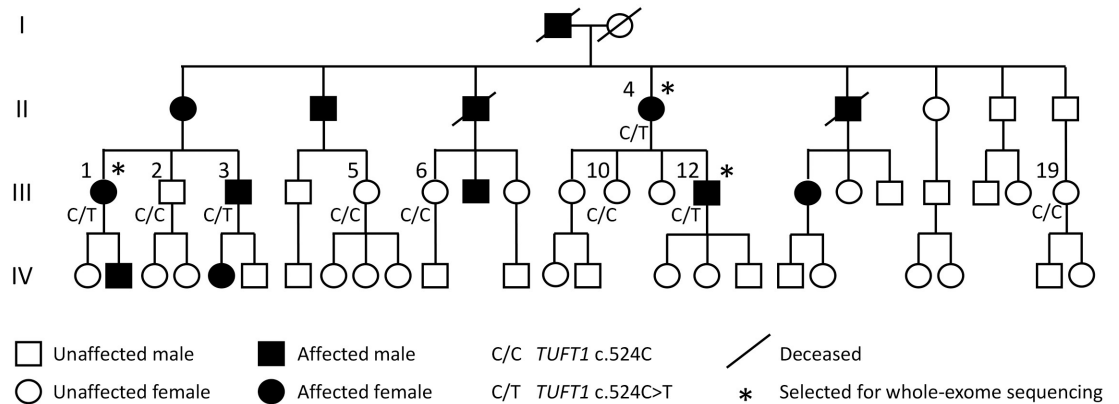


Fig 1. The pedigree of the Finnish MTP I OA family and the *TUFT1* c.524C>T segregation. The numbering indicates individuals whose DNA was available for the study. The *TUFT1* genotype is indicated below each individual. The pedigree is modified from Nissi *et al.* 2011 [15].

<https://doi.org/10.1371/journal.pone.0175474.g001>

the only variant perfectly co-segregating with the MTP I OA in the family. The variant introduces a threonine to methionine substitution at position 175 (p.Thr175Met, NP_064512).

Detection of Copy Number Variations (CNVs)

CNVs calls were generated from exome data to screen possible structural genome variations such as deletions and duplications. Altogether 160 CNVs were called in chromosomes 1–22. Of these, 142 were deletions and 18 were amplifications. The three affected family members had a mutual CNV region on chromosome 17 where two patients (II-4 and III-1) showed a heterozygous deletion and one patient (III-2) had an amplification (data not shown). Annotation to the Database of Genomic Variants showed that this region has been previously reported to be a common CNV region [24].

The effect of c.524C>T on mRNA and protein expression

The function of the identified variant was studied *in vitro* in human embryonic kidney (HEK293) cells. Cells transfected with the mutant *TUFT1* construct (HEK293-mutTUFT1) generated less ($P \leq 0.001$) *TUFT1* mRNA than cells transfected with the wt *TUFT1* construct (HEK293-wtTUFT1, Fig 2A). Consistent with this, the variant attenuated tuftelin protein expression (Fig 2B and S1 Fig).

Table 1. Summary statistics for exome sequence data analysis steps.

	SNV count	Indel count
Autosomal variants shared by the three affected family members	48 860	4 670
Shared by the affected family members, not found in the controls	5 794	525
Novel and rare variants (MAF \leq 0.01 or unknown)	739	366
Exonic or splicing	143	12
Harmful <i>in silico</i> prediction	33	5
Co-segregates with MTP I OA*	1	0

SNV, single nucleotide variant; indel, insertions and deletions,
*validation by Sanger sequencing in nine family members.

<https://doi.org/10.1371/journal.pone.0175474.t001>

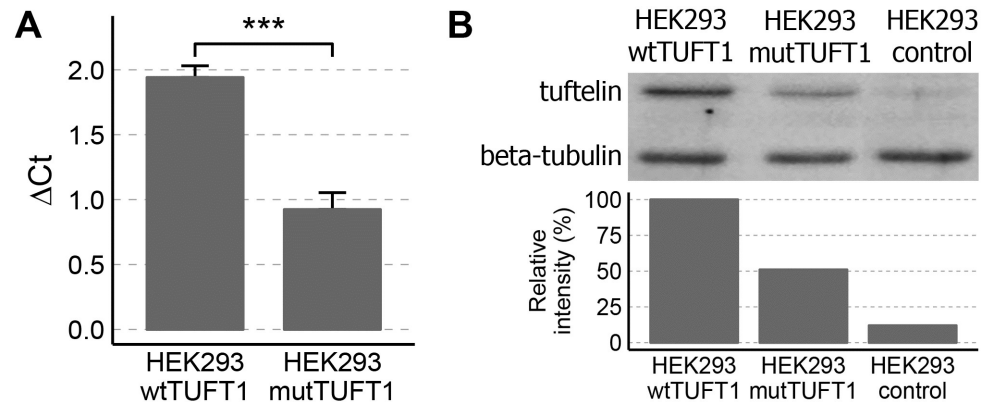


Fig 2. The effect of the c.524C>T variant on *TUFT1* expression in *TUFT1* overexpressing HEK293 cells. (A) *TUFT1* mRNA expression in HEK293-mutTUFT1 cells was approximately 47% of the expression observed in HEK293-wtTUFT1 cells (***) $P \leq 0.001$. *ACTB* and *B2M* were used as reference genes. (B) The variant suppressed also tuftelin protein expression, as the relative intensity of tuftelin in HEK293-mutTUFT1 cells was 51% of the relative intensity of tuftelin observed in HEK293-wtTUFT1 cells. The relative intensities were calculated from the ratio of tuftelin to beta-tubulin absolute intensities. The faint band in the control cells corresponds to the endogenous tuftelin recognized by the antibody.

<https://doi.org/10.1371/journal.pone.0175474.g002>

The role of *TUFT1* overexpression in chondrocyte differentiation

To study the functional role of tuftelin in chondrogenesis and mineralization, ATDC5 cells stably overexpressing wt or mutant tuftelin (ATDC5-wtTUFT1 or ATDC5-mutTUFT1, respectively) and empty vector controls (ATDC5-ctrl) were grown in calcifying conditions in the presence of insulin, ascorbic acid and beta-glycerophosphate (β GP) for 15 days. Expression of three marker genes for chondrogenic differentiation, sex determining region Y-box 9 (*Sox9*), type II collagen (*Col2a1*), aggrecan (*Agc1*), and four marker genes for chondrocyte hypertrophy, runt-related transcription factor 2 (*Runx2*), type X collagen (*Col10a1*), matrix metalloproteinase 13 (*Mmp13*), and alkaline phosphatase (*Alpl*) were studied at three time points using real-time quantitative polymerase chain reaction (qPCR).

Overexpression of both wt and mutant *TUFT1* significantly influenced the expression of *Col2a1* and *Agc1* ($P = 2.95 \times 10^{-15}$ and $P = 1.86 \times 10^{-12}$, respectively, Fig 3A, S2 Table), but did not affect the expression of *Sox9* ($P = 0.461$, Fig 3A, S2 Table): in ATDC5-mutTUFT1 cells *Col2a1* expression differed from control cells on all the measurement days whereas in ATDC5-wtTUFT1 cells the difference reached statistical significance on days 8 and 15 (S3 Table). Additionally, *Col2a1* expression was significantly lower in ATDC5-mutTUFT1 cells in comparison to ATDC5-wtTUFT1 cells on days 12 and 15 ($P = 0.008$ and $P = 0.045$, respectively, Fig 3A, S3 Table). *Agc1* expression in both ATDC5-mutTUFT1 and ATDC5-wtTUFT1 cells deviated from the expression seen in control cells, while there was no statistically significant difference between the mutant and wt cells (S3 Table).

No statistically significant differences were observed in the *Runx2* expression on any of the days (Fig 3B, S3 Table). *Col10a1* expression showed a similar trend in ATDC5-ctrl and ATDC5-wtTUFT1 cells. On day 15 expression of *Col10a1* in the ATDC5-mutTUFT1 cells was significantly lower when compared to the ATDC5-wtTUFT1 cells ($P = 0.007$, Fig 3B, S3 Table). The expression of *Mmp13* was significantly lower in both ATDC5-wtTUFT1 and ATDC5-mutTUFT1 cells in comparison to the control cells on day 15 ($P = 2.09 \times 10^{-5}$ and $P = 0.011$, Fig 3B, S3 Table). The expression of *Alpl* in ATDC5-mutTUFT1 cells was significantly higher in control cells already on day eight ($P = 0.005$, Fig 3B, S3 Table), whereas on day

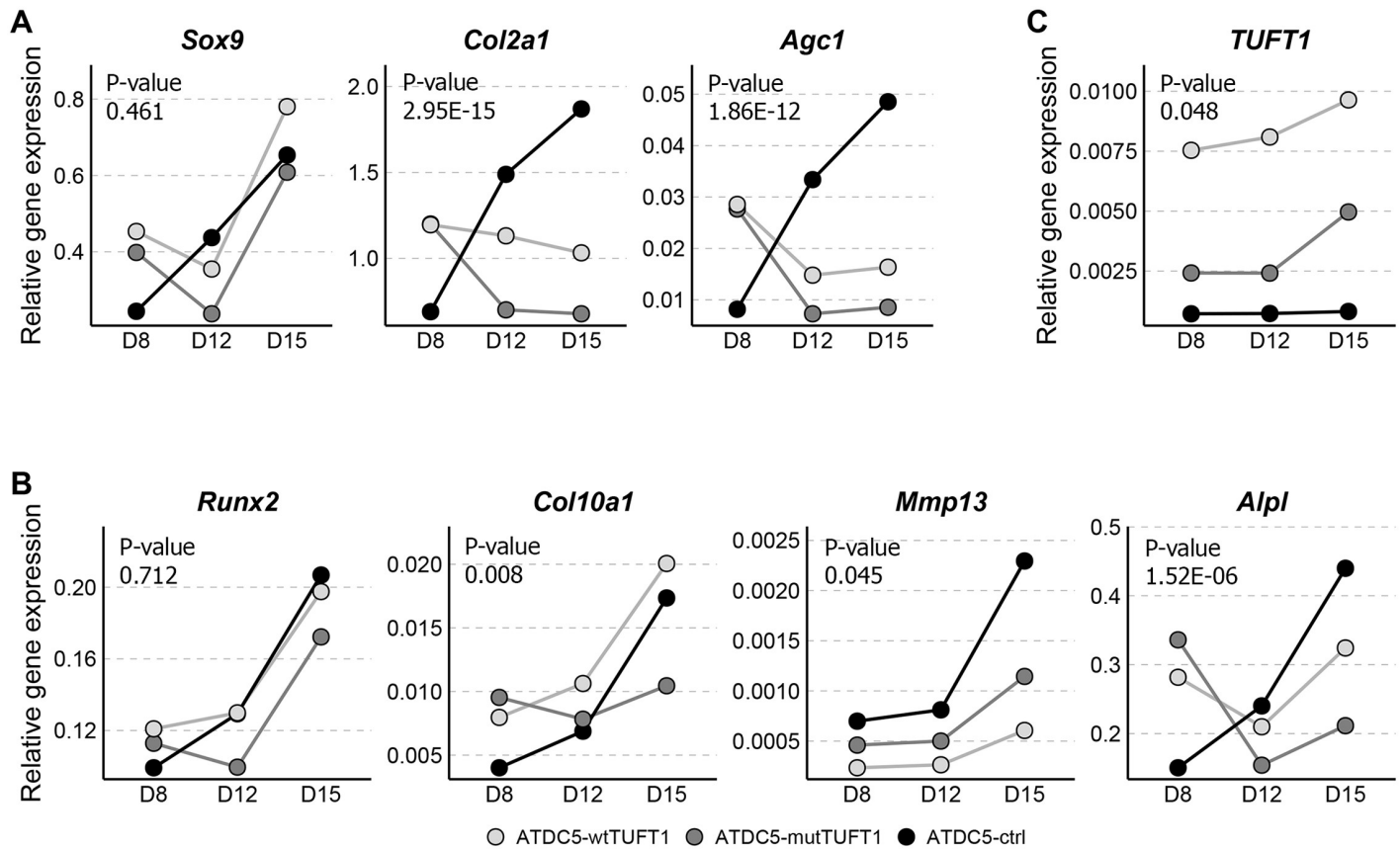


Fig 3. Expression of chondrocyte differentiation and hypertrophy marker genes, and *TUFT1* in ATDC5 cells. (A) *Sox9*, *Col2a1*, and *Agc1* are markers for chondrocyte differentiation and (B) *Runx2*, *Col10a1*, *Mmp13*, and *Alpl* markers for chondrocyte hypertrophy. In addition, expression of *TUFT1* was determined (C). Expressions were studied by real-time qPCR in mixed population clones overexpressing wt or mutant *TUFT1* (ATDC5-wtTUFT1, ATDC5-mutTUFT1) and in empty vector controls (ATDC5-ctrl) at three time points during 15 days of differentiation. *Hprt* and *Ppia* were used as reference genes. Results are represented as means of three groups of quadruplet samples and relative gene expression denotes log(x+1) transformed fold changes. P-values relate to the confidence of whether the change in the relative gene expression over time is different between the ATDC5-wtTUFT1, ATDC5-mutTUFT1 and ATDC5-ctrl cell populations (S2 Table).

<https://doi.org/10.1371/journal.pone.0175474.g003>

15 the *Alpl* expression in ATDC5-mutTUFT1 cells was significantly lower than in control cells ($P = 2.12 \times 10^{-4}$, Fig 3B, S3 Table).

Expression of *TUFT1* was assessed at three time points (Fig 3C). Comparable with the study done in HEK293 cells, *TUFT1* expression was lower in the ATDC5-mutTUFT1 cells than in the ATDC5-wtTUFT1 cells at all time points. All three cell populations showed an increasing trend of *TUFT1* expression during the 15-day period. Results of gene expression studies in ATDC5 cells are presented in Fig 3, and the test statistics are summarized in S2 and S3 Tables.

Contribution of *TUFT1* overexpression to extracellular matrix mineralization and nodule formation

Calcium and proteoglycan content in the extracellular matrix (ECM) of the ATDC5 cells were studied at three time points along the 15-day culture period using Alizarin red and Alcian blue stainings, respectively. In general, the contents of both calcium (Fig 4A) and proteoglycans (Fig 4B) in the ECM of both ATDC5-mutTUFT1 and ATDC5-wtTUFT1 cells deviated from what was seen in control cells at the three time points. The most evident deviation was the significant increase in the calcium content in the ECM of ATDC5-mutTUFT1 cells on day 15

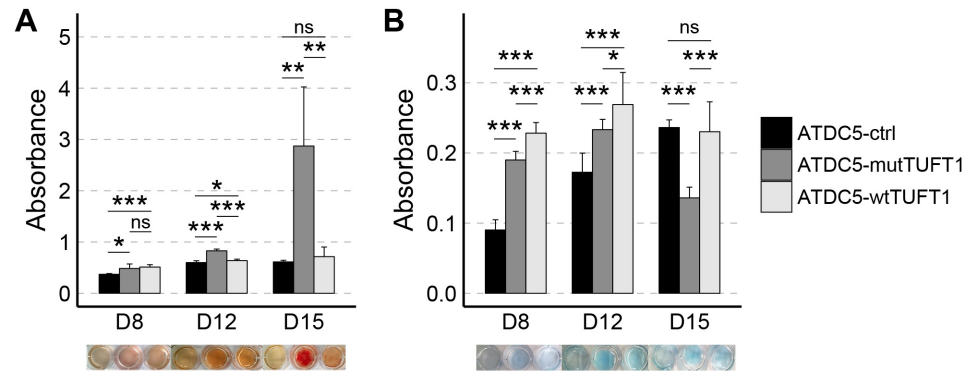


Fig 4. ECM mineralization in ATDC5-ctrl, ATDC5-mutTUFT1 and ATDC5-wtTUFT1 cells during differentiation. (A) Calcium content was visualized by Alizarin red staining and (B) proteoglycan content by Alcian blue staining. The staining was quantified by spectrophotometer at 570 nm and 630 nm, respectively. Measurements were performed on the days 8, 12 and 15 and results are represented as mean \pm standard deviation of four wells analyzed. Abbreviations: ns, not significant; * $P \leq 0.05$; ** $P \leq 0.01$; *** $P \leq 0.001$.

<https://doi.org/10.1371/journal.pone.0175474.g004>

(Fig 4A). On the contrary on day 15 the ATDC5-mutTUFT1 cells showed reduced amount of proteoglycans in the ECM when compared with the control and ATDC5-wtTUFT1 cells (Fig 4B).

During the differentiation experiment, control cells begin to form cartilaginous nodules and ECM mineralization centres, seen as concentrated black deposits in Fig 5A. Nodule formation in ATDC5-wtTUFT1 cells was impaired when compared with control cells, and no mineralization centres were observed (Fig 5B). Nodule formation was also impaired in the ATDC5-mutTUFT1 cells and mineralization occurred disorderly throughout the cell culture (Fig 5C) compatible with the observed increase in the ECM calcium (Fig 4A).

Discussion

In the present study we identified a rare nonsynonymous variant (rs41310883, c.524C>T, p.Thr175Met) in *TUFT1* that co-segregates with MTP I OA in a Finnish family. *TUFT1* encodes tuftelin protein which plays a role in enamel mineralization [16,17], but is also suggested to have a more universal function due to its wide expression in multiple cell and tissue types [18–20]. Our *in vitro* experiments showed that the c.524C>T variant decreased both *TUFT1* mRNA and tuftelin protein expression in *TUFT1* overexpressing HEK293 cells, and

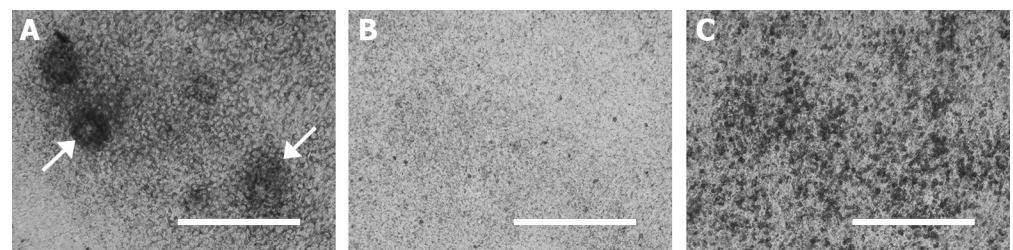


Fig 5. Formation of mineralizing cartilage nodules in ATDC5 cells overexpressing *TUFT1* *in vitro*. (A) Control cells formed mineralizing cartilage nodules (arrow), seen as centred opaque deposits in the microscopic images taken on day 15 of differentiation. (B) Nodule and mineralization center formation was diminished in ATDC5-wtTUFT1 cells. (C) Nodule formation was impaired also in ATDC5-mutTUFT1 cells and mineralization occurred in a disordered manner throughout the culture. The scale bar represents 400 μ m.

<https://doi.org/10.1371/journal.pone.0175474.g005>

altered the calcium and proteoglycan content in the ECM of ATDC5 cells. Interestingly, overexpression of both wt and mutant *TUFT1* in ATDC5 cells altered chondrogenic differentiation, as indicated by atypical expression of differentiation marker genes and diminished formation of cartilage nodules. Our findings suggest that *TUFT1* plays a role in chondrocyte differentiation and cartilage mineralization apparently on a calcium-related pathway, and the identified variant likely contributes to the disease phenotype in the studied family by giving rise to cartilage ECM modifications often seen in association with OA.

The identified c.524C>T variant was found to alter the amount of calcium and proteoglycans in the ECM of ATDC5 cells over a 15-day culture period suggesting that the mutation alters cell functions involved in the assembly of ECM. Particularly the highly increased extracellular calcium on day 15 was the distinguishable feature that seemed to be due to the c.524C>T variant rather than due to *TUFT1* overexpression. The variant introduces an amino acid residue that is larger in size and more hydrophobic than the wt residue likely disrupting proper folding of the protein [25]. The mutation also resides in one of the two coiled-coil domains in tuftelin which may also contribute to altered function of tuftelin, as coiled-coil domains are important for proper protein folding and known to be crucial in multiple biological functions [26]. Furthermore, the mutation locates on one of tuftelin's ten evolutionarily conserved phosphorylation sites that are predicted to function in chelation of calcium [27]. The observed effect of the mutation could be due to tuftelin's altered affinity to calcium or due to improper folding disturbing protein-protein interactions or due to both of these. Increased calcification and degraded proteoglycans are distinctive features of osteoarthritic cartilage [5,28], and therefore it seems likely that the identified mutation is involved in the pathogenesis of the MTP I OA in the studied family.

Seemingly *TUFT1* overexpression alone is sufficient to interfere with chondrogenesis, as we discovered that in addition to ATDC5-mut*TUFT1* cells chondrogenic differentiation was diminished also in ATDC5-wt*TUFT1* cells. Both of the cell populations showed a decreasing trend of chondrogenic differentiation marker genes *Col2a1* and *Agc1* during the 15-day culture period while in the control cells the expression strengthened over time, as expected. In addition, in the beginning of chondrogenesis mesenchymal precursor cells should start to condensate to form nodules [29], whereas we observed that the nodule formation was diminished in both of the *TUFT1* overexpressing ATDC5 cell populations. This advocates that proper timing and/or quantity of *TUFT1* expression is crucial for the differentiation to proceed appropriately. Similar findings were obtained in a study done on mice, which indicated that tuftelin overexpression disturbed the growth of carbonated calcium hydroxyapatite crystallites in developing enamel and the phenotype was most evident in mice with the greatest tuftelin expression [30].

Tuftelin appears to function at the very beginning of the differentiation process: we observed that the differentiation marker gene expression as well as the ECM mineralization in both ATDC5-mut*TUFT1* and ATDC5-wt*TUFT1* cells deviates from what is seen in the control cells already on day eight. A highly similar phenotype with impaired marker gene expression and diminished nodule formation during differentiation has previously been described in mouse chondrocytes with inactivated *Sox9* [31,32]. However, we did not detect significant difference in the expression of *Sox9* between the ATDC5-mut*TUFT1*, ATDC5-wt*TUFT1* and ATDC5-ctrl cells suggesting that the described phenotype arises downstream from *Sox9* expression. We hypothesize that *TUFT1* overexpression inhibits differentiation signaling downstream from *Sox9* by altering cells' calcium metabolism. This could further interfere the normal function of calcium-dependent adhesion molecule N-cadherin which is expressed in the early chondrogenesis following *Sox9* expression, but prior to expression of *Col2a1* and *Agc1* [33]. During chondrogenesis N-cadherin plays a role in cell aggregation [34,35] an event which has been proposed to be a crucial step in the early phase of the differentiation cascade,

influencing also *COL2A1* expression *in vitro* in chick chondrocytes [36]. Assessing the effect of the identified mutation in relation to the function of N-cadherin could be an interesting topic for further studies.

This study has some limitations. Whole exome sequencing allows us to detect only the coding and surrounding region variants, while non-coding variations are missed. Regulatory regions locating in non-coding intronic and intergenic regions have been associated with OA (11) as well as with many other complex diseases [37–39]. However, it has been estimated that approximately 85% of mutations with large phenotypic effects are located on protein coding regions, and thus Mendelian traits result most often from exonic or splice-site mutations [40]. Another limitation is that only one family was available to the study. Unfortunately, population samples available from the same geographical area as the studied family, such as the Northern Finland Birth Cohorts (NFBC, <http://www.oulu.fi/nfbc/>), do not provide a suitable phenotype (radiographically determined arthritis of the first metatarsophalangeal joint) to perform a population level replication, nor does the chip-based genotype data from NFBC allow replication of rare variants, as they are excluded from the data for technical reasons. Disease symptoms limited to the MTP I joint may partially be explained by joint loading or site specific methylation profiles [41,42]. An animal model could inform more on tuftelin's function during development of MTP I OA, but would be challenging to implement due the specific characteristics of human foot anatomy and impact of physical loading and environmental factors on the disease phenotype. A genome editing method, such as CRISPR-Cas9, would need to be applied to generate a mouse model with the specific *TUFT1* mutation, as *TUFT1* knockout mice do not display deformities in joints, bones or enamel [43]. A genome editing method could be also applied to generate an *in vitro* model that would help to better distinguish the effect of the identified mutation from *TUFT1* overexpression.

Results of the present study implicate that *TUFT1* plays a role in chondrocyte differentiation and cartilage mineralization apparently on a calcium-related pathway, and thus can be considered as a novel susceptibility gene for MTP I OA. Our findings also advocate that investigation of rare variants and familial forms of complex phenotypes can provide valuable information about pathogenic mechanisms behind common diseases, such as OA. Further studies are needed to determine whether *TUFT1* variants associate to cartilage phenotypes on population level and to elucidate the precise biological function of tuftelin in chondrogenesis and mineralization of cartilage.

Materials and methods

Subjects

This study was approved by the Ethical Committee of the Northern Ostrobothnia Hospital District and a written consent was obtained from the study participants. Nissi *et al.* (2011) reported a Finnish family where early-onset MTP I OA is inherited in an autosomal dominant manner [15]. Thirteen out of 52 family members were affected (Fig 1). The mean age of onset was 26, ranging from 12 to 51. The radiological findings are described in detail by Nissi *et al.* [15]. Briefly, the X-ray images of the affected family members revealed typical OA related findings in the first MTP joint including joint space narrowing, subchondral sclerosis, osteophyte and cyst formation. Otherwise the other joints of the feet were healthy and there was no evidence of erosive lesions. No other deformities in the skeletal body were detected and large joints were not affected even in the older family members. Affected family members were otherwise healthy and had normal body height and weight. Also, individuals participating to the present study did not display any self-reported dental phenotype.

All the family members were contacted and interviewed. Four patients (II-4, III-1, III-3, III-12) having symptomatic and radiographic bilateral OA in addition to five asymptomatic family members (III-2, III-5, III-6, III-10, III-19) were willing to participate to the study.

Whole exome sequencing

Three affected family members (II-4, III-1 and III-12) were selected for exome sequencing. In addition, two unrelated individuals were exome sequenced and used as control samples in the variant filtering steps. Blood samples were obtained from the participants and DNA was extracted using standard protocols. Exome sequencing and variant calling were done at the Institute for Molecular Medicine Finland (FIMM). Exonic sequences were enriched using the NimbleGen SeqCap EZ Human Exome Library v2.0 (Roche, NimbleGen, Inc., Madison, USA), and sequencing was done using a High Seq 2000 platform (Illumina, San Diego, USA). To ensure the quality of the variants, the exome data were taken through the FIMM bioinformatics pipeline [44].

Variant annotation and filtering

Exome sequence data was filtered based on three assumptions. The causal variant was assumed to fit to the autosomal dominant model of inheritance as appeared in the pedigree. Furthermore, the causal variant(s) was/were presumed to be *de novo* or rare, since to our knowledge no similar families were previously described in the literature. Penetrance was assumed to be 100%, and therefore all the individuals having the disease genotype were presumed to be symptomatic. Variant filtering was done in R by selecting the variants shared by the affected family members and then excluding the variants found in the two unrelated control samples. Next, the variants previously not annotated into the Single Nucleotide Polymorphism Database 135 (dbSNP135), rare variants according to the 1000 Genomes Project (minor allele frequency ≤ 0.01) and variants with a record in dbSNP but with unknown frequency were annotated using ANNOVAR [45]. Exonic variants with harmful prediction by SIFT [46], PolyPhen 2 [47] or MutationTaster [48] algorithms and variants located at splice sites were considered harmful and chosen for further validation.

Variant validation using Sanger sequencing

The selected variants were genotyped in all family members with DNA available using Sanger sequencing. Primers used in Sanger sequencing were designed using Primer3 v0.4.0 [49]. Primer sequences and PCR conditions are available on request. Purified PCR products were sequenced using ABI3500xL Genetic Analyzer and BigDye Terminator vs.1.1 reagents (Life Technologies, Carlsbad, USA). The results were analyzed using Variant Reporter version 2.0 (Life Technologies, Carlsbad, USA).

Detection of CNVs

Detection of CNVs from whole exome data was done using a read count based CNV caller cn.MOPS [50]. CNVs regions shared by the samples were annotated using Database of Genomic Variants [51] to identify common CNVs.

TUFT1 constructs

A *TUFT1* cDNA clone was obtained from GenScript and cloned into pcDNA3.1 (-) expression vector (Invitrogen, Carlsbad, USA) using BamHI and XbaI restriction enzymes. The *TUFT1* variant c.524C>T was generated using QuikChange Site-Directed Mutagenesis Kit

(Stratagene, San Diego, USA) according to the manufacturer's instructions. All sequences were confirmed by capillary sequencing.

Cell culture and transfections

HEK293 cells were cultured and maintained in DMEM with 10% FBS and plated in 10cm-plates at a density of 2×10^6 cells/plate for protein analyses and in 6-well plates at a density of 3.5×10^5 cells/well for real-time qPCR analyses 24h prior to transient transfections. Transfections for protein and qPCR analysis were performed using 5.6 μ g DNA (wt or mutant *TUFT1* construct) and 40 μ l FuGENE HD transfection reagent (Promega, Madison, USA) or 2 μ g DNA and 14 μ l FuGENE HD transfection reagent, respectively.

Mouse ATDC5 cells are widely used to model of chondrogenic differentiation and subsequent mineralization [52,53]. We applied a model for ATDC5 cells developed by Newton *et al.* allowing us to study chondrogenesis and ECM mineralization in a 15-day period [54]. ATDC5 cells (Sigma, St Louis, USA) were cultured in maintenance medium DMEM/F-12 (1:1) with GlutaMAX I (Gibco, Paisley, Scotland) containing 5% FBS, 1% sodium pyruvate, 0,1% penicillin (Sigma, St Louis, USA) and 0,01% Fungizone (Cambrex Bio Science, Walkersville, MD). For stable transfections 3.5×10^5 cells/well were plated on six-well plates and transfected at a ratio of 7:2 FuGENE HD transfection reagent (Promega, Madison, USA) to 2 μ l of DNA according to the manufacturer's instructions. Empty pcDNA3.1 (-) was used as a control. After 24h the medium was replaced with fresh maintenance medium supplemented with 500 μ g/ml Geneticin, G418 (Sigma, St Louis, USA). The selection medium was changed every second or third day until all of the cells without the neomycin resistance gene on the on a separate control plate were killed. Cell death was evaluated using light microscopy (Leica Microsystems, Wetzlar, Germany). A mixed population of stable G418 transfectants was expanded and cultured in differentiation medium (maintenance medium supplemented with 1x insulin-transferrin-selenium, 500 μ g/ml Geneticin). The cells were plated in 24-well plates at a density of 5.0×10^4 cells/ml. After the cells had reached confluency, 50 μ g/ml ascorbic acid and 10 mM β GP were added and the cells were incubated in a humidified atmosphere (37°C, 5% CO₂) for 15 days.

During differentiation chondrocytes are expected to form mineralizing cartilage nodules that can be detected as opaque deposits in microscopy images [54,55]. Nodule formation of ATDC5 was determined, and pictures were taken after 15 days of differentiation using EVOS fluorescence microscope.

Real-time qPCR

Preceding to qPCR, total RNA was extracted from cells using an E.Z.N.A Total RNA Kit (Omega Bio-Tek, Norcross, USA) with RNase-free DNase (Omega Bio-Tek, Norcross, USA) treatment and cDNA was synthesized using 1 μ g RNA per sample using an iScript cDNA Synthesis Kit (Bio-Rad, Hercules, USA). The effect of the c.524C>T on *TUFT1* expression was studied in HEK293 cells at one time point from three duplicate samples using an iTaq Universal SYBR Green Supermix kit (Bio-Rad, Hercules, USA) according to the manufacturer's instructions in a CFX96 Real-Time System (Bio-Rad, Hercules, USA). Δ Ct was determined by using *ACTB* (beta actin) and *B2M* (beta-2-microglobulin) as reference genes.

In chondrogenic differentiation mesenchymal progenitor cells proliferate and differentiate into chondrocytes. During this step, chondrocytes express *Sox9* transcription factor and number of cartilage matrix genes, including *Col2a1* and *Agc1*. This is followed by endochondral ossification when chondrocytes lose their differentiated phenotype, and became hypertrophic and mature chondrocytes. In this phase cells start to express matrix metalloproteinase 13, a

cartilage degrading enzyme encoded by *Mmp13*, alkaline phosphatase (*Alpl*) which is an important enzyme for mineralization, runt related transcription factor 2 (*Runx2*) involved in regulation of skeletal gene expression and type X collagen (*Col10a1*), a specific marker for hypertrophic chondrocytes (reviewed in [56] and [57]). To analyze the expression of these chondrogenic and hypertrophic markers in chondrocytes, a real-time qPCR was carried out on four samples in duplicate on days 8, 12 and 15 and three technical repeats were performed. The gene expression levels were determined by the comparative C_T ($2^{-\Delta\Delta C_T}$) method [58] using *Hprt* (hypoxanthine guanine phosphoribosyl transferase) and *Ppia* (peptidylprolyl isomerase A) as reference genes.

Oligonucleotide primers used in real-time qPCR amplification are listed in S4 Table. For each primer no template controls were included in duplicate.

Preparation of cell lysates and Western blotting

After 48h of culturing, the growth media of HEK293 cells transiently transfected with wt or mutant *TUFT1* were collected (cell medium fraction, CM) and the cells were washed with ice cold phosphate buffered saline (PBS). Buffer 1 (10 mM Hepes (pH 7.9), 10 mM KCl, 1.5 mM MgCl₂, 0.1 mM EDTA, 0.1 mM EGTA, 0.1% TritonX-100, 1 mM DTT, 1 × protease inhibitor (cOmplete ULTRA Tablets, mini, Roche, Mannheim, Germany)) was added to the plates and the cells were scraped off. Next, the cells were incubated 30 min with constant agitation at 4°C. The samples were centrifuged and the supernatants were collected (cytosolic fraction, CF). The pellet was washed with PBS and the cells were resuspended in buffer 2 (20 mM Hepes (pH 7.9), 400 mM NaCl, 0.25 mM EGTA, 1.5 mM MgCl₂, 10% glycerol, 0.5 mM DTT, 1 × protease inhibitor (cOmplete ULTRA Tablets, mini, Roche, Mannheim, Germany)) and incubated a further 20 min with constant agitation at 4°C. The samples were centrifuged and supernatants collected (nuclear fraction, NF).

To analyze the effect of the c.524C>T on tuftelin expression and localization, 12.5% sodium dodecyl sulfate polyacrylamide gel electrophoresis (SDS-PAGE) gels were prepared. For electrophoresis 1 µg of total protein was analyzed under reducing conditions. Proteins separated on the gels were transferred onto polyvinylidene difluoride membranes (Millipore, Bedford, USA), which were blocked with 1×TBS (50 mM Tris-Cl, 150 mM NaCl, pH 7.5) with 0.05% Tween 20 (Merck, Darmstadt, Germany) containing 5% non-fat dry milk and probed with the primary antibody (1:2000 Anti-TUFT1 (86–100) antibody produced in rabbit (Sigma, St Louis, USA) in 1×TBS). Anti-beta Tubulin produced in rabbit (Abcam, Cambridge, UK) was used as a loading control. To visualize the immune complex 1:10 000 Anti-Rabbit IgG—Peroxidase antibody produced in goat in 1×TBS (Sigma, St Louis, USA) was used. The imaging of Western blot membranes was performed using Luminescent Image Analyzer LAS-3000 (FUJIFILM Medical Systems, USA) and the signal densities were quantified using ImageJ 1.47v (National Institutes of Health, USA).

Histochemical staining of ATDC5 cells

Calcium and proteoglycan content of mixed populations of ATDC5-ctrl, ATDC5-wtTUFT1, and ATDC5-mutTUFT1 cells were determined by staining the cell layers with Alizarin red stain (Sigma, St Louis, USA) or Alcian blue stain (Sigma, St Louis, USA), respectively. Cells were grown 15 days after their mineralization state was analyzed. To evaluate calcium concentration, ATDC5 cells were fixed with 4% paraformaldehyde (PFA) for 5 min at 4°C, washed with PBS, stained with 2% Alizarin red (pH 4.2) for 5 min in room temperature, washed with distilled water and bound dye was extracted with 10% cetylpyridium chloride for 10 min. Optical density (OD) of the samples was determined at 570 nm by spectrophotometry.

Proteoglycan content was analyzed by washing ATDC5 cells with PBS, fixing with 95% methanol for 20 min, staining with 1% Alcian blue 8GX (Sigma, St Louis, USA) in 0.1M HCl overnight and rinsing with distilled water. Cell cultures were extracted with 6M guanidine-HCl for 6h at room temperature and the released dye was evaluated by measuring the OD at 630 nm by spectrophotometer.

Statistical analysis

Differences in *TUFT1* expression in HEK293 cells as well as in ECM mineralization characterized by Alizarin red Alcian blue stainings were analyzed using Student's t-test. Differences in marker gene expressions between ATDC5-ctrl, ATDC5-wtTUFT1, and ATDC5-mutTUFT1 cells were determined using repeated measurements analysis of variance (ANOVA) followed by Tukey's Honest Significant Difference (HSD) *post hoc* test. Prior to ANOVA and Tukey HSD, fold changes were $\log(x+1)$ transformed. P-values smaller than 0.05 were considered statistically significant in all the analyses. Statistical analyses were performed using Microsoft Excel 2013 (Student's t-test for *TUFT1* expression in HEK293 cells) and R version 3.2.2. (repeated measurement ANOVA, Tukey HSD and Student's t-test for ECM mineralization).

Supporting information

S1 Fig. The original uncropped Western blot image. 1 μ g of total protein was used in the preparation of Western blot. Anti-TUFT1 and Anti-beta Tubulin primary antibodies and Anti-Rabbit IgG—Peroxidase secondary antibody were used in the experiment. (TIF)

S1 Table. Variants selected for validation by Sanger sequencing. (DOCX)

S2 Table. Expression of marker genes for chondrocyte differentiation and hypertrophy (real-time qPCR): Repeated measurements ANOVA. Measurements were done separately for ATDC5-ctrl, ATDC5-wtTUFT1 and ATDC5-mutTUFT1 cell populations (CELL) at three time points (DAY). CELL:DAY interaction indicates whether the relative gene expression level changes over time in differing manner in the three cell populations. * $P \leq 0.05$; ** $P \leq 0.01$; *** $P \leq 0.001$. (DOCX)

S3 Table. Expression of marker genes for chondrocyte differentiation and hypertrophy (real-time qPCR): Tukey HSD. Pairwise comparisons of the marker gene expression levels in the three cell populations at the three time points. (DOCX)

S4 Table. Primers used in qPCR analyses. (DOCX)

Acknowledgments

We are grateful to the family for their participation to this study. The authors would like to acknowledge Dr. Anu Laitala for her valuable advice in *in vitro* analyses. Anu Myllymäki and Aira Erkkilä are thanked for the excellent technical help.

Author Contributions

Conceptualization: MM RN MT ES JI.

Formal analysis: ES MT MW SS.

Funding acquisition: MM.

Investigation: ES MT MW SS VA LR.

Methodology: MT ES LR.

Project administration: MM MT ES.

Resources: RN JI.

Supervision: MM LR.

Visualization: MT ES.

Writing – original draft: MT ES MW SS.

Writing – review & editing: MM LR.

References

1. Johnson VL, Hunter DJ. The epidemiology of osteoarthritis. *Best Pract Res Clin Rheumatol* 2014 Feb; 28(1):5–15. <https://doi.org/10.1016/j.berh.2014.01.004> PMID: 24792942
2. Loeser RF, Goldring SR, Scanzello CR, Goldring MB. Osteoarthritis: a disease of the joint as an organ. *Arthritis Rheum* 2012 Jun; 64(6):1697–1707. <https://doi.org/10.1002/art.34453> PMID: 22392533
3. Arden N, Nevitt MC. Osteoarthritis: epidemiology. *Best Pract Res Clin Rheumatol* 2006 Feb; 20(1):3–25. <https://doi.org/10.1016/j.berh.2005.09.007> PMID: 16483904
4. Kean WF, Kean R, Buchanan WW. Osteoarthritis: symptoms, signs and source of pain. *Inflammopharmacology* 2004; 12(1):3–31. <https://doi.org/10.1163/156856004773121347> PMID: 15035776
5. Goldring MB, Marcu KB. Cartilage homeostasis in health and rheumatic diseases. *Arthritis Res Ther* 2009; 11(3):224. <https://doi.org/10.1186/ar2592> PMID: 19519926
6. Karlson EW, Mandl LA, Aweh GN, Sangha O, Liang MH, Grodstein F. Total hip replacement due to osteoarthritis: the importance of age, obesity, and other modifiable risk factors. *Am J Med* 2003 Feb 1; 114(2):93–98. PMID: 12586227
7. Spector TD, Cicuttini F, Baker J, Loughlin J, Hart D. Genetic influences on osteoarthritis in women: a twin study. *BMJ* 1996 Apr 13; 312(7036):940–943. PMID: 8616305
8. Meulenbelt I, Bijkerk C, Breedveld FC, Slagboom PE. Genetic linkage analysis of 14 candidate gene loci in a family with autosomal dominant osteoarthritis without dysplasia. *J Med Genet* 1997 Dec; 34(12):1024–1027. PMID: 9429149
9. Ingvarsson T, Stefansson SE, Gulcher JR, Jonsson HH, Jonsson H, Frigge ML, et al. A large Icelandic family with early osteoarthritis of the hip associated with a susceptibility locus on chromosome 16p. *Arthritis Rheum* 2001 Nov; 44(11):2548–2555. PMID: 11710711
10. Jakkula E, Melkonien M, Kiviranta I, Lohiniva J, Raina SS, Perala M, et al. The role of sequence variations within the genes encoding collagen II, IX and XI in non-syndromic, early-onset osteoarthritis. *Osteoarthritis Cartilage* 2005 Jun; 13(6):497–507. <https://doi.org/10.1016/j.joca.2005.02.005> PMID: 15922184
11. Taipale M, Jakkula E, Kamarainen OP, Gao P, Skarp S, Barral S, et al. Targeted re-sequencing of linkage region on 2q21 identifies a novel functional variant for hip and knee osteoarthritis. *Osteoarthritis Cartilage* 2016 Apr; 24(4):655–663. <https://doi.org/10.1016/j.joca.2015.10.019> PMID: 26603474
12. Iagnocco A, Rizzo C, Gattamelata A, Vavala C, Ceccarelli F, Cravotto E, et al. Osteoarthritis of the foot: a review of the current state of knowledge. *Med Ultrason* 2013 Mar; 15(1):35–40. PMID: 23486622
13. Trivedi B, Marshall M, Belcher J, Roddy E. A systematic review of radiographic definitions of foot osteoarthritis in population-based studies. *Osteoarthritis Cartilage* 2010 Aug; 18(8):1027–1035. <https://doi.org/10.1016/j.joca.2010.05.005> PMID: 20472083
14. Bergin SM, Munteanu SE, Zammit GV, Nikolopoulos N, Menz HB. Impact of first metatarsophalangeal joint osteoarthritis on health-related quality of life. *Arthritis Care Res (Hoboken)* 2012 Nov; 64(11):1691–1698.
15. Nissi R, Perhomaa M, Silvennoinen L, Halonen V, Rasila R, Winblad I, et al. Hereditary isolated metatarsophalangeal arthritis. *Scand J Rheumatol* 2011 Jan; 40(1):22–25. <https://doi.org/10.3109/03009742.2010.495081> PMID: 20858143

16. Deutsch D, Palmon A, Fisher LW, Kolodny N, Termine JD, Young MF. Sequencing of bovine enamelin ("tuftelin") a novel acidic enamel protein. *J Biol Chem* 1991 Aug 25; 266(24):16021–16028. PMID: [1874744](#)
17. Shaffer JR, Carlson JC, Stanley BO, Feingold E, Cooper M, Vanyukov MM, et al. Effects of enamel matrix genes on dental caries are moderated by fluoride exposures. *Hum Genet* 2015 Feb; 134(2):159–167. <https://doi.org/10.1007/s00439-014-1504-7> PMID: [25373699](#)
18. MacDougall M, Simmons D, Dodds A, Knight C, Luan X, Zeichner-David M, et al. Cloning, characterization, and tissue expression pattern of mouse tuftelin cDNA. *J Dent Res* 1998 Dec; 77(12):1970–1978. <https://doi.org/10.1177/00220345980770120401> PMID: [9839784](#)
19. Mao Z, Shay B, Hekmati M, Fermon E, Taylor A, Dafni L, et al. The human tuftelin gene: cloning and characterization. *Gene* 2001 Nov 28; 279(2):181–196. PMID: [11733143](#)
20. Saarikoski ST, Rivera SP, Hankinson O. Mitogen-inducible gene 6 (MIG-6), adipophilin and tuftelin are inducible by hypoxia. *FEBS Lett* 2002 Oct 23; 530(1–3):186–190. PMID: [12387890](#)
21. Mori Y, Chung UI, Tanaka S, Saito T. Determination of differential gene expression profiles in superficial and deeper zones of mature rat articular cartilage using RNA sequencing of laser microdissected tissue specimens. *Biomed Res* 2014; 35(4):263–270. PMID: [25152035](#)
22. Leiser Y, Silverstein N, Blumenfeld A, Shilo D, Haze A, Rosenfeld E, et al. The induction of tuftelin expression in PC12 cell line during hypoxia and NGF-induced differentiation. *J Cell Physiol* 2011 Jan; 226(1):165–172. <https://doi.org/10.1002/jcp.22318> PMID: [20658530](#)
23. Oliveira FS, Bellesini LS, Defino HL, da Silva Herrero CF, Beloti MM, Rosa AL. Hedgehog signaling and osteoblast gene expression are regulated by purmorphamine in human mesenchymal stem cells. *J Cell Biochem* 2012 Jan; 113(1):204–208. <https://doi.org/10.1002/jcb.23345> PMID: [21898541](#)
24. Park H, Kim JI, Ju YS, Gokcumen O, Mills RE, Kim S, et al. Discovery of common Asian copy number variants using integrated high-resolution array CGH and massively parallel DNA sequencing. *Nat Genet* 2010 May; 42(5):400–405. <https://doi.org/10.1038/ng.555> PMID: [20364138](#)
25. Venselaar H, Te Beek TA, Kuipers RK, Hekkelman ML, Vriend G. Protein structure analysis of mutations causing inheritable diseases. An e-Science approach with life scientist friendly interfaces. *BMC Bioinformatics* 2010 Nov 8; 11:548-2105-11-548.
26. Burkhard P, Stetefeld J, Strelkov SV. Coiled coils: a highly versatile protein folding motif. *Trends Cell Biol* 2001 Feb; 11(2):82–88. PMID: [11166216](#)
27. Deutsch D, Leiser Y, Shay B, Fermon E, Taylor A, Rosenfeld E, et al. The human tuftelin gene and the expression of tuftelin in mineralizing and nonmineralizing tissues. *Connect Tissue Res* 2002; 43(2–3):425–434. PMID: [12489194](#)
28. Ea HK, Nguyen C, Bazin D, Bianchi A, Guicheux J, Reboul P, et al. Articular cartilage calcification in osteoarthritis: insights into crystal-induced stress. *Arthritis Rheum* 2011 Jan; 63(1):10–18. <https://doi.org/10.1002/art.27761> PMID: [20862682](#)
29. DeLise AM, Fischer L, Tuan RS. Cellular interactions and signaling in cartilage development. *Osteoarthritis Cartilage* 2000 Sep; 8(5):309–334. <https://doi.org/10.1053/joca.1999.0306> PMID: [10966838](#)
30. Luo W, Wen X, Wang HJ, MacDougall M, Snead ML, Paine ML. In vivo overexpression of tuftelin in the enamel organic matrix. *Cells Tissues Organs* 2004; 177(4):212–220. <https://doi.org/10.1159/000080134> PMID: [15459477](#)
31. Bi W, Deng JM, Zhang Z, Behringer RR, de Crombrughe B. Sox9 is required for cartilage formation. *Nat Genet* 1999 May; 22(1):85–89. <https://doi.org/10.1038/8792> PMID: [10319868](#)
32. de Crombrughe B, Lefebvre V, Behringer RR, Bi W, Murakami S, Huang W. Transcriptional mechanisms of chondrocyte differentiation. *Matrix Biol* 2000 Sep; 19(5):389–394. PMID: [10980415](#)
33. Stanton LA, Underhill TM, Beier F. MAP kinases in chondrocyte differentiation. *Dev Biol* 2003 Nov 15; 263(2):165–175. PMID: [14597193](#)
34. Oberlander SA, Tuan RS. Expression and functional involvement of N-cadherin in embryonic limb chondrogenesis. *Development* 1994 Jan; 120(1):177–187. PMID: [8119125](#)
35. Delise AM, Tuan RS. Analysis of N-cadherin function in limb mesenchymal chondrogenesis in vitro. *Dev Dyn* 2002 Oct; 225(2):195–204. <https://doi.org/10.1002/dvdy.10151> PMID: [12242719](#)
36. Tacchetti C, Tavella S, Dozin B, Quarto R, Robino G, Cancedda R. Cell condensation in chondrogenic differentiation. *Exp Cell Res* 1992 May; 200(1):26–33. PMID: [1563490](#)
37. Gaulton KJ, Nammo T, Pasquali L, Simon JM, Giresi PG, Fogarty MP, et al. A map of open chromatin in human pancreatic islets. *Nat Genet* 2010 Mar; 42(3):255–259. <https://doi.org/10.1038/ng.530> PMID: [20118932](#)

38. Musunuru K, Strong A, Frank-Kamenetsky M, Lee NE, Ahfeldt T, Sachs KV, et al. From noncoding variant to phenotype via SORT1 at the 1p13 cholesterol locus. *Nature* 2010 Aug 5; 466(7307):714–719. <https://doi.org/10.1038/nature09266> PMID: 20686566
39. Westra HJ, Peters MJ, Esko T, Yaghootkar H, Schurmann C, Kettunen J, et al. Systematic identification of trans eQTLs as putative drivers of known disease associations. *Nat Genet* 2013 Oct; 45(10):1238–1243. <https://doi.org/10.1038/ng.2756> PMID: 24013639
40. Majewski J, Schwartzenruber J, Lalonde E, Montpetit A, Jabado N. What can exome sequencing do for you? *J Med Genet* 2011 Sep; 48(9):580–589. <https://doi.org/10.1136/jmedgenet-2011-100223> PMID: 21730106
41. Schibler L, Gibbs L, Benoist-Lasselin C, Decraene C, Martinovic J, Loget P, et al. New insight on FGFR3-related chondrodysplasias molecular physiopathology revealed by human chondrocyte gene expression profiling. *PLoS One* 2009 Oct 29; 4(10):e7633. <https://doi.org/10.1371/journal.pone.0007633> PMID: 19898608
42. Smith R. Mechanical loading effects on articular cartilage matrix metabolism and osteoarthritis. In: Buckwalter JA, Lotz MK & Stolz JF (eds) *Osteoarthritis, Inflammation and Degradation: A Continuum*. 2007; Amsterdam, IOS Press: 14–23.
43. Eppig JT, Blake JA, Bult CJ, Kadin JA, Richardson JE, Mouse Genome Database Group. The Mouse Genome Database (MGD): facilitating mouse as a model for human biology and disease. *Nucleic Acids Res* 2015 Jan; 43(Database issue):D726–36. <https://doi.org/10.1093/nar/gku967> PMID: 25348401
44. Sulonen AM, Ellonen P, Almusa H, Lepisto M, Eldfors S, Hannula S, et al. Comparison of solution-based exome capture methods for next generation sequencing. *Genome Biol* 2011 Sep 28; 12(9):R94-2011-12-9-r94.
45. Wang K, Li M, Hakonarson H. ANNOVAR: functional annotation of genetic variants from high-throughput sequencing data. *Nucleic Acids Res* 2010 Sep; 38(16):e164. <https://doi.org/10.1093/nar/gkq603> PMID: 20601685
46. Ng PC, Henikoff S. Predicting deleterious amino acid substitutions. *Genome Res* 2001 May; 11(5):863–874. <https://doi.org/10.1101/gr.176601> PMID: 11337480
47. Adzhubei IA, Schmidt S, Peshkin L, Ramensky VE, Gerasimova A, Bork P, et al. A method and server for predicting damaging missense mutations. *Nat Methods* 2010 Apr; 7(4):248–249. <https://doi.org/10.1038/nmeth0410-248> PMID: 20354512
48. Schwarz JM, Rodelsperger C, Schuelke M, Seelow D. MutationTaster evaluates disease-causing potential of sequence alterations. *Nat Methods* 2010 Aug; 7(8):575–576. <https://doi.org/10.1038/nmeth0810-575> PMID: 20676075
49. Koressaar T, Remm M. Enhancements and modifications of primer design program Primer3. *Bioinformatics* 2007 May 15; 23(10):1289–1291. <https://doi.org/10.1093/bioinformatics/btm091> PMID: 17379693
50. Klambauer G, Schwarzbauer K, Mayr A, Clevert DA, Mitterecker A, Bodenhofer U, et al. cn.MOPS: mixture of Poissons for discovering copy number variations in next-generation sequencing data with a low false discovery rate. *Nucleic Acids Res* 2012 May; 40(9):e69. <https://doi.org/10.1093/nar/gks003> PMID: 22302147
51. MacDonald JR, Ziman R, Yuen RK, Feuk L, Scherer SW. The Database of Genomic Variants: a curated collection of structural variation in the human genome. *Nucleic Acids Res* 2014 Jan; 42(Database issue):D986–92. <https://doi.org/10.1093/nar/gkt958> PMID: 24174537
52. Shukunami C, Ishizeki K, Atsumi T, Ohta Y, Suzuki F, Hiraki Y. Cellular hypertrophy and calcification of embryonal carcinoma-derived chondrogenic cell line ATDC5 in vitro. *J Bone Miner Res* 1997 Aug; 12(8):1174–1188. <https://doi.org/10.1359/jbmr.1997.12.8.1174> PMID: 9258747
53. Fujita T, Meguro T, Izumo N, Yasutomi C, Fukuyama R, Nakamura H, et al. Phosphate stimulates differentiation and mineralization of the chondroprogenitor clone ATDC5. *Jpn J Pharmacol* 2001 Mar; 85(3):278–281. PMID: 11325020
54. Newton PT, Staines KA, Spevak L, Boskey AL, Teixeira CC, Macrae VE, et al. Chondrogenic ATDC5 cells: an optimised model for rapid and physiological matrix mineralisation. *Int J Mol Med* 2012 Nov; 30(5):1187–1193. <https://doi.org/10.3892/ijmm.2012.1114> PMID: 22941229
55. Shukunami C, Ishizeki K, Atsumi T, Ohta Y, Suzuki F, Hiraki Y. Cellular hypertrophy and calcification of embryonal carcinoma-derived chondrogenic cell line ATDC5 in vitro. *J Bone Miner Res* 1997 Aug; 12(8):1174–1188. <https://doi.org/10.1359/jbmr.1997.12.8.1174> PMID: 9258747
56. Kronenberg HM. Developmental regulation of the growth plate. *Nature* 2003 May 15; 423(6937):332–336. <https://doi.org/10.1038/nature01657> PMID: 12748651

57. Mackie EJ, Ahmed YA, Tatarczuch L, Chen KS, Mirams M. Endochondral ossification: how cartilage is converted into bone in the developing skeleton. *Int J Biochem Cell Biol* 2008; 40(1):46–62. <https://doi.org/10.1016/j.biocel.2007.06.009> PMID: [17659995](https://pubmed.ncbi.nlm.nih.gov/17659995/)
58. Schmittgen TD, Livak KJ. Analyzing real-time PCR data by the comparative C(T) method. *Nat Protoc* 2008; 3(6):1101–1108. PMID: [18546601](https://pubmed.ncbi.nlm.nih.gov/18546601/)